

- to be melted by transient shocks.
25. J. Fernández and W.-H. Ip, *Icarus* **47**, 470 (1981); *ibid.* **58**, 109 (1984).
  26. We used the Bulirsch-Stoer algorithm [R. Bulirsch and J. Stoer, *Numer. Math.* **8**, 1 (1966)]. We assumed a gas density of  $10^{-10}$  g cm $^{-3}$ , with fractional deviation from Keplerian rotation  $5 \times 10^{-3}$ . Planetesimals were assumed to have density 2 g cm $^{-3}$  and drag coefficient of 0.4.
  27. S. Dermott and C. Murray, *Nature* **301**, 201 (1983); M. J. Holman and N. W. Murray, *Astron. J.* **112**, 1278 (1996).
  28. For small eccentricity, orbital decay is primarily due to the non-Keplerian rotation of the nebula. If the eccentricity is large compared with the fractional deviation from the Kepler velocity, there is an additional secular decay of the semimajor axis as well as damping of inclination; see Adachi *et al.* (17).
  29. F. Podosek and P. Cassen, *Meteoritics* **29**, 6 (1994).
  30. Our cases were computed in three dimensions, with initial inclinations between 0° and 1°. There was no significant increase in mean inclination during evolution in resonance.
  31. F. Whipple, in *Physical Studies of Minor Planets*, T. Gehrels, Ed. (NASA SP-267, 1971), p. 251.
  32. The resonance angle for the  $p:q$  resonance is  $p\lambda_j - q\lambda_p - \bar{\omega}$ , where  $\lambda_j$  and  $\lambda_p$  are the mean longitudes of Jupiter and the planetesimal, and  $\bar{\omega}$  is the planetesimal's longitude of perihelion; see F. Marzari, H. Scholl, L. Tomasella, and V. Vanzani [*Planet. Space*

*Sci.* **45**, 337 (1997)].

33. Beyond 3.5 AU, the asteroid belt is dominated by low-albedo objects believed to consist of primitive, organic-rich material. Some examples of these types are found in the inner belt [J. C. Gradie, C. R. Chapman, E. F. Tedesco, in *Asteroids II*, R. Binzel, T. Gehrels, M. Matthews, Eds. (Univ. of Arizona Press, Tucson, 1989), p. 316].
34. G. W. Wetherill, *Icarus* **100**, 307 (1992).
35. We thank T. Swindle, T. V. Ruzmaikina, and J. A. Wood for discussions. Supported by NASA (S.J.W. and L.L.H.) and the Italian Space Agency (F.M.). This is Planetary Science Institute Contribution 343.

29 September 1997; accepted 5 December 1997

## Possible Production of High-Energy Gamma Rays from Proton Acceleration in the Extragalactic Radio Source Markarian 501

K. Mannheim

The active galaxy Markarian 501 was discovered with air-Cerenkov telescopes at photon energies of 10 tera-electron volts. Such high energies may indicate that the gamma rays from Markarian 501 are due to the acceleration of protons rather than electrons. Furthermore, the observed absence of gamma ray attenuation due to electron-positron pair production in collisions with cosmic infrared photons implies a limit of 2 to 4 nanowatts per square meter per steradian for the energy flux of an extragalactic infrared radiation background at a wavelength of 25 micrometers. This limit provides important clues about the epoch of galaxy formation.

Gamma rays ( $\gamma$  rays) from cosmic sources impinging on Earth's atmosphere initiate electromagnetic showers in which the energy of the primary  $\gamma$  ray is imparted among secondary electron-positron pairs. The blue Cerenkov light emitted by the pairs in the atmosphere can be detected from the ground with optical telescopes triggering on the short ( $\sim 1$  ns) optical pulses. The technique has advanced considerably in recent years (1), and some surprising discoveries have been made. Among them is the detection of the blazar Markarian 501 (Mrk 501) at energies above 10 TeV (1 TeV =  $10^{12}$  eV) (2).

Blazars are remote but very powerful sources characterized by their variable polarized synchrotron emission. They are associated with radio jets (bipolar outflows) emerging from giant elliptical galaxies seen at small angles with the line of sight. Mrk 501 is  $\sim 3 \times 10^8$  light-years from Earth but nevertheless produces a tera-electron volt  $\gamma$  ray flux during outbursts that is many times stronger than that of the Crab Nebula, a supernova remnant inside our Milky Way at a distance of only  $6 \times 10^3$  light-years. The radiation mechanism responsible for the  $\gamma$  rays could be

either inverse Compton scattering of low-energy photons by accelerated electrons (3) or pion production by accelerated protons. In the latter case, the sources could be among the long-sought sources of cosmic rays; that is, the isotropic flux of relativistic particles with differential number density ( $N$ ) spectrum  $dN/dE \propto E^{-2.7}$  (for energies  $E < 10^3$  TeV), mainly consisting of protons and ions (4).

Particle acceleration in astrophysics is typically observed to be associated with (collisionless) shock waves when a supersonic flow of magnetized material hits a surrounding medium. Examples of shock waves are shell-type supernova remnants (explosion of a massive star), plerions (pulsar wind),  $\gamma$  ray bursts (relativistic ejecta from the collapse of a compact stellar object), or the jets ejected from active galactic nuclei (collimated relativistic wind from the accretion disk around a supermassive black hole).

In the theoretical picture of shock acceleration, relativistic particles (protons, ions, and electrons) scatter elastically off turbulent fluctuations in the magnetic field on both sides of the shock and thereby gain energy because of the convergence of the scattering centers (approaching walls). The acceleration time scale for the process can be written as  $t_{\text{acc}} = \xi r_g c/v^2$ , where  $v$  denotes

the velocity of the shock wave ( $c$  is the speed of light) and  $r_g \propto E/B$  denotes the radius of gyration of a particle with energy  $E$  in a magnetic field of strength  $B$ . The effects of shock obliquity, turbulence spectrum, and other unknowns are conveniently hidden in an empirical factor  $\xi \geq 1$ . The most rapid (gyro-time scale) particle acceleration for relativistic shocks corresponds to  $\xi = 1$  (5). Balancing the acceleration time scale with the energy loss time scale due to synchrotron radiation  $t_{\text{syn}} \propto B^{-2} E^{-1}$ , one obtains the maximum energy of the electrons  $E_{\text{max}} = 10 (\xi/10)^{-0.5} (B/3\mu\text{G})^{-0.5} (v/10^8 \text{ cm s}^{-1})$  TeV (6). The observed 10-TeV  $\gamma$  rays from the Crab Nebula (7) and the observed synchrotron x-rays in shell-type supernova remnants (8) (corresponding to 10-TeV electrons) require  $\xi \sim 1$  to 10. Because protons lose less energy, they can reach larger  $E_{\text{max}}$ 's than electrons and give rise to  $\gamma$  ray emission even above  $\sim 10$  TeV by means of pion production and subsequent pion decay. Although shock acceleration theory predicts that most of the cosmic rays are accelerated in supernova remnants (4), no definitive  $\gamma$  ray signature has yet been discovered.

It has been argued that the assumption of electron acceleration also suffices to explain the  $\gamma$  rays from blazar jets such as Mrk 501 (9). Estimates of the magnetic field strength in the  $\gamma$  ray-emitting part of the jet in Mrk 501 then yield values in the range  $B \sim 0.04$  to 0.7 G. This magnetic field is much stronger than the one in supernova remnants, and the associated stronger cooling of the relativistic electrons due to synchrotron energy losses reduces  $E_{\text{max}}$  accordingly. The effect is almost compensated for by the high shock wave velocities in extragalactic radio sources, which speed up the acceleration rate. Using radio interferometry, shock wave velocities close to the speed of light have been inferred, corresponding to typical bulk Lorentz factors in the range  $\Gamma_{\text{jet}} = (1 - \beta^2)^{-0.5} \sim 2$  to 10 ( $\beta = v/c$ ), with a few cases of still higher values (10). Because of the alignment of the jet axis and the line of sight in Mrk 501, superluminal motion has not been observed.

Universitäts-Sternwarte, Geismarlandstraße 11, Göttingen D-37083, Germany. E-mail: kmannhe@uni-sw.gwdg.de

With  $v = c$ ,  $\xi = 10$ , and taking into account equal synchrotron and inverse Compton losses, one obtains  $E_{\text{max}} \sim 4 \Gamma_{\text{jet}}(B/G)^{-0.5}$  TeV from the balance between acceleration gains and energy losses. The additional factor  $\Gamma_{\text{jet}}$  takes into account the boost in energy due to the relativistic bulk motion. Therefore, electron maximum energies of  $\sim 10$  TeV as required for Mrk 501 [at least 5 to 8 TeV are required for the similar blazar Mrk 421 (11)] are formally allowed, but one certainly has to push the theory to its limits and this raises a number of concerns. (i) The multi-TeV spectrum should show considerable curvature because of the (so-called Klein-Nishina) decrease of the scattering cross section when the energy of the scattered photon approaches  $E_{\text{max}}$  and because of the onset of electron-positron pair production (the observed multi-TeV spectrum is consistent with a smooth power law). (ii) The ratio between the  $\gamma$  ray and synchrotron (simultaneous) luminosities depends sensitively on the jet Lorentz factor  $\Gamma_{\text{jet}}$  and therefore requires fine tuning (both nearest bright blazars, Mrk 421 and Mrk 501, show a similar  $\gamma$ -to- $x$ -ray luminosity ratio). (iii) The magnetic field pressure turns out to be much lower than the relativistic electron pressure in the electron acceleration models, which seems inconsistent with the shock acceleration mechanism (the turbulent magnetic field is responsible for pushing the electrons back and forth across the shock); larger values of  $B$  are also expected from the adiabatic expansion of a magnetically collimated jet [the observed  $B$  field at the tips of the jet in Cygnus A is consistent with adiabatic expansion (12)]. (iv) Larger values of  $\Gamma_{\text{jet}}$  could ameliorate the problem that  $E_{\text{max}} \sim 10$  TeV; however, one would run into a problem with unification models of active galaxies if  $\Gamma_{\text{jet}} > 10$  were the rule rather than the exception (13) (the number of required host galaxies would exceed the number of known radio galaxies).

A natural solution to the problem is to assume that the 10-TeV  $\gamma$  rays are due to pion production from accelerated protons. The balance equation between energy gains and losses for protons yields maximum energies of  $\sim 10^6$  TeV and short variability time scales  $t_{\text{var}} \geq 10^5(\xi/\Gamma_{\text{jet}})(B/G)^{-1}$  seconds in Mrk 501 (14). The relativistic proton energy loss is dominated by photoproduction of pions in collisions with low-energy synchrotron photons (originating from accelerated electrons). Collisions of the accelerated protons with matter are negligible because of the low density of matter in relativistic jets [unless a high-density target moves across the jet (15)]. The  $\gamma$  rays from the decay of the neutral pion (far above the observed range of ener-

gies) are subject to pair creation in further collisions with the low-energy synchrotron photons ( $\gamma + \gamma \rightarrow e^+ + e^-$ ). This initiates an electromagnetic cascade, shifting the average photon energy to the tera-electron volt range and below. A model based on the combined acceleration of protons ( $\gamma$  rays) and electrons (radio-to- $x$ -rays)—called the proton blazar model (16)—was fitted to published data of Mrk 501 in order to obtain a prediction of its multi-TeV spectrum (17). Data from 1995 and earlier were available for the analysis and covered the radio-to- $x$ -ray wavelength range, including a flux limit above 100 MeV and an integral flux above 300 GeV [for details see references in (17)]. The published flux values showed considerable variability in the optical-to- $x$ -ray range, and the model spectrum was therefore fitted to match the time-averaged spectrum (from the fit, one obtains  $B = 37$  G and  $\Gamma_{\text{jet}} = 10$ ). The predicted multi-TeV spectrum is shown in Fig. 1 and compared with the data obtained from recent (1996 and 1997) air-Cerenkov observations. The fairly robust spectral slope of the model spectrum fits the observations, whereas the absolute flux normalization is somewhat too low. Considering that the sub-TeV (350 GeV) flux has been reported to increase from 1995 to 1997 (9), the agreement is actually rather impressive if one scales up the model spectrum accordingly. Contemporaneous multi-wavelength observations of blazars such as Mrk 501 will be important to discriminate between electron-based and proton-based models for the  $\gamma$  ray emission from them. Generally, electron-based models require larger values of  $\Gamma_{\text{jet}}$  and lower values of  $B$  to obtain high-energy  $\gamma$  rays than do proton-based models.

There is a further hint that proton acceleration might be important. Unresolved blazars are the most probable source population to produce the observed extragalactic  $\gamma$  ray background between 10 MeV and 10 GeV (18). The energy density of this  $\gamma$  ray background is  $\approx 4 \times 10^{-6}$  eV cm $^{-3}$ . A similar value is found for an extragalactic flux of protons (with  $dN/dE \propto E^{-2}$  differential spectrum between  $10^9$  and  $10^{20}$  eV) providing all of the observed cosmic rays with energies above  $10^{18.5}$  eV (the so-called “ankle” above which the very-high-energy differential cosmic ray spectrum  $\propto E^{-3}$  flattens) (19). On the assumption that the  $\gamma$  rays are from proton ( $p$ ) acceleration, the comparable energy densities result from simple decay kinematics: Photoproduction of neutral pions ( $\pi^0$ ) ( $p + \gamma \rightarrow \pi^0 + p$ ) and their subsequent decay give rise to  $\gamma$  rays (subject to electromagnetic cascading), which carry  $\sim 1/5$  of the proton energy. Charged pions ( $p + \gamma \rightarrow \pi^+ + n$ ) are produced at approximately the same rate and give rise to neutrons ( $n$ ),

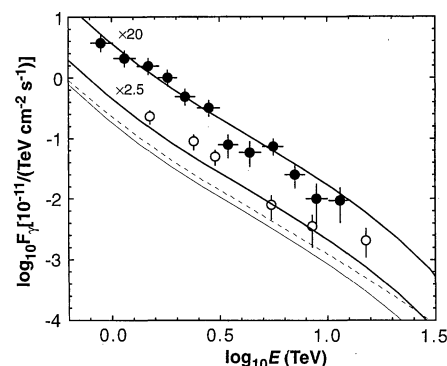


**Fig. 1.** Differential TeV spectrum of Mrk 501. Thin solid line: proton blazar model prediction based on archival data from 1995 and earlier (17) taking into account intergalactic attenuation adopting a DIRB spectrum based on a cold + hot dark matter model of galaxy formation from (23) with  $v_v$  ( $25 \mu\text{m}$ ) =  $1.0 \text{ nW m}^{-2} \text{ sr}^{-1}$  and a Hubble constant  $H_0 = 75 \text{ km s}^{-1} \text{ Mpc}^{-1}$  (throughout the paper). Thin dashed line: same as thin solid line, without intergalactic attenuation. Thick solid lines: model spectrum scaled up by factors of 2.5 and 20, corresponding to the increase in the mean sub-TeV flux from 1995 to 1996 and the spring of 1997, respectively (9). Open circles: HEGRA (High-Energy Gamma-Ray Astronomy) CT1 observation March to August 1996 (220 hours) (27). Solid circles: HEGRA IACT observation March to April 1997 (26.7 hours) (2).

which carry  $\sim 4/5$  of the accelerated proton energy. Because the neutrons do not scatter off the magnetic field fluctuations responsible for the acceleration and storage of the charged particles in the blazar jet, they must escape the accelerator (energy losses are small and modify the neutron spectrum only at the very highest energies). Time dilation allows the most energetic neutrons to leave the host galaxy freely before  $\beta$  decay occurs (for protons there would be adiabatic losses due to the magnetic field in the host galaxy). Hence the neutron (and after  $\beta$  decay the proton) luminosity is equal to the  $\gamma$  ray luminosity within factors of order unity. An extragalactic origin of the highest energy cosmic rays is indeed suggested by the absence of an enhancement of the cosmic ray flux toward the galactic disk (20) and by the change in chemical composition from heavy (protons and ions) to light (protons) above  $10^{18.5}$  eV (21). The ultimate challenge to the hypothesis is the measurement of the high-energy neutrino ( $\nu$ ) flux associated with the charged pion decay ( $\pi^\pm \rightarrow e^\pm + 3\nu$ ). The energy density in these multi-TeV neutrinos would be of the same order of magnitude as that in extragalactic cosmic rays and  $\gamma$  rays. Their measurement therefore constitutes an experimentum crucis that is within reach for the planned cubic kilometer underwater (ice) detectors (22).

Although  $\gamma$  rays are known from labo-

ratory experiments for their penetrating power, propagation over intergalactic distances is not without hurdles. A diffuse isotropic infrared background (DIRB) was produced when the first galaxies formed. Massive stars in early galaxies produced large amounts of dust in their winds, re-processing the visual and ultraviolet light from the stars into infrared (IR) light. By colliding with these ample IR photons,  $\gamma$  ray photons can disappear and turn into electron-positron pairs (23–25). The most numerous IR photons above the threshold for pair production with 10-TeV  $\gamma$  rays have wavelengths  $\sim 25 \mu\text{m}$ . The mean free path ( $\lambda_{\gamma\gamma}$ ) for pair creation at multi-TeV energies is of the order of the distance  $d$  of Mrk 501. The exact value depends on the DIRB, which is difficult to measure directly because of the presence of zodiacal light and galactic cirrus clouds.

One can use the observed power law spectrum (2) to put a limit on the maximum allowed pair attenuation, assuming that the observed power law is the unattenuated spectrum emitted by the source (consistent with the proton-based model). In general, only contrived intrinsic spectra would look like a smooth power law after the quasi-exponential attenuation. The maximum allowed deviation from the power law  $[1 - \exp(-d/\lambda_{\gamma\gamma})]$  is taken to be the size of the statistical error bar at 10 TeV, yielding an optical depth  $\tau_{\gamma\gamma} = d/\lambda_{\gamma\gamma} < 0.7$ . This limit can be relaxed by a factor not larger than  $\sim 2$ , admitting for weakly absorbed spectra that still approximate a power law (dashed line in Fig. 1). There is some dependence of the attenuation on the shape of the DIRB spectrum. Useful models for the spectral shape can be found in (23–25) and yield a similar limit for the 25- $\mu\text{m}$  DIRB normalization  $\nu I_{\nu}$  ( $25 \mu\text{m}$ )  $< (2 \text{ to } 4) \text{ nW m}^{-2} \text{ sr}^{-1}$ . The absence of  $\gamma$  ray attenuation in Mrk 501 is consistent with no contribution to the DIRB other than from the optically selected galaxies, for which one expects  $\sim 10\%$  of their optical emission to be reprocessed by warm dust, yielding  $\nu I_{\nu}$  ( $25 \mu\text{m}$ )  $\sim 1 \text{ nW m}^{-2} \text{ sr}^{-1}$  (26), but would also allow a DIRB that is stronger by a factor of 2 to 4. A DIRB of at least  $\sim 3 \text{ nW m}^{-2} \text{ sr}^{-1}$  is suggested by faint IR galaxy counts and indicates contributions from dust-en-shrouded galaxies at red shifts of  $z \sim 3$  to 4 (24). Electron-based models for the  $\gamma$  ray emission from Mrk 501 (9) predict deviations from a power law in the multi-TeV range even without external attenuation and therefore impose an upper limit on the DIRB that is below the lower limit from faint IR galaxy counts. If both methods of estimating the DIRB (deviations from a power law spectrum in the multi-

TeV range and faint IR galaxy counts) use correct assumptions, a cutoff in the  $\gamma$  ray spectrum of Mrk 501 must be present in the energy range 10 to 30 TeV.

## REFERENCES AND NOTES

1. M. F. Cawley and T. C. Weekes, *Exp. Astron.* **6**, 7 (1995).
2. F. Aharonian *et al.*, *Astron. Astrophys.* **327**, L5 (1997).
3. C. D. Dermer and R. Schlickeiser, *Science* **257**, 1642 (1992).
4. P. O. Lagage and C. J. Cesarsky, *Astron. Astrophys.* **125**, 249 (1983); B. Wiebel-Sooth, P. L. Biermann, H. Meyer, *ibid.*, in press.
5. J. R. Jokipii, *Astrophys. J.* **313**, 842 (1987); J. Bednartz and M. Ostrowski, *Mon. Not. R. Astron. Soc.* **283**, 447 (1996).
6. S. R. Reynolds, *Astrophys. J.* **459**, L13 (1996).
7. O. C. De Jager *et al.*, *ibid.* **457**, 253 (1996).
8. K. Koyama *et al.*, *Nature* **378**, 255 (1995).
9. M. Catanese *et al.*, *Astrophys. J.* **487**, L143 (1997); J. Quinn *et al.*, *ibid.* **456**, L83 (1996); E. Pian *et al.*, *Astrophys. J. Lett.*, in press.
10. G. Ghisellini, P. Padovani, A. Celotti, L. Maraschi, *Astrophys. J.* **407**, 65 (1993).
11. F. Krennrich *et al.*, *ibid.* **481**, 758 (1997).
12. D. E. Harris, C. L. Carilli, R. A. Perley, *Nature* **367**, 713 (1994).
13. C. M. Urry and P. Padovani, *Pub. Astron. Soc. Pacific* **107**, 803 (1995).
14. P. L. Biermann and P. A. Strittmatter, *Astrophys. J.* **322**, 643 (1987).
15. A. Dar and A. Laor, *ibid.* **478**, L5 (1997).
16. K. Mannheim, P. L. Biermann, W. M. Krüß, *Astron. Astrophys.* **251**, 723 (1991); K. Mannheim, *ibid.* **269**, 67 (1993).
17. K. Mannheim, S. Westerhoff, H. Meyer, H.-H. Fink, *ibid.* **315**, 77 (1996).
18. D. A. Kniffen *et al.*, *Astron. Astrophys. Suppl.* **120**, 615 (1996); P. Padovani, G. Ghisellini, A. C. Fabian, A. Celotti, *Mon. Not. R. Astron. Soc.* **260**, L21 (1993); C. Impey, *Astron. J.* **112**, 2667 (1996).
19. R. J. Protheroe and P. A. Johnson, *Astroparticle Phys.* **5**, 215 (1996).
20. T. Stanev, P. L. Biermann, J. Lloyd-Evans, J. P. Rachen, A. A. Watson, *Phys. Rev. Lett.* **75**, 3065 (1995).
21. J. P. Rachen, T. Stanev, P. L. Biermann, *Astron. Astrophys.* **273**, 377 (1993); N. Hayashida *et al.*, *Phys. Rev. Lett.* **77**, 1000 (1996).
22. T. K. Gaisser, F. Halzen, T. Stanev, *Phys. Rep.* **258**, 173 (1995).
23. D. MacMinn and J. R. Primack, *Space Sci. Rev.* **75**, 413 (1996).
24. A. Franceschini *et al.*, *Astron. Astrophys. Suppl.* **89**, 285 (1991); A. Franceschini *et al.*, in *ESA FIRST Symposium* (European Space Agency special publication 401), in press; T. Stanev and A. Franceschini, in preparation.
25. F. W. Stecker and M. A. Malkan, *Astrophys. J.*, in press.
26. P. Madau *et al.*, *Mon. Not. R. Astron. Soc.* **283**, 1388 (1996); B. T. Soifer and G. Neugebauer, *Astron. J.* **101**, 354 (1991).
27. D. Petry *et al.*, in *Proceedings of the 25th International Cosmic Ray Conference*, Durban, South Africa, August 1997, P. A. Evenson *et al.*, Eds. (International Union of Pure and Applied Physics, in press); S. M. Bradbury *et al.*, *Astron. Astrophys.* **320**, L5 (1997).
28. I thank P. Biermann, A. Dar, J. Kirk, H. Meyer, J. Primack, W. Rhode, F. Rieger, and the referees for their critical reading and suggestions for improvement of the manuscript. This research was generously supported by the Deutsche Forschungsgemeinschaft under travel grant DFG/Ma 1545/6-1.

3 September 1997; accepted 25 November 1997

## Bragg Diffraction from Crystallized Ion Plasmas

W. M. Itano,\* J. J. Bollinger, J. N. Tan,† B. Jelenković,‡  
X.-P. Huang, D. J. Wineland

Single crystals of a one-component plasma were observed by optical Bragg diffraction. The plasmas contained  $10^5$  to  $10^6$  single-positive beryllium-9 ions ( ${}^9\text{Be}^+$ ) at particle densities of  $10^8$  to  $10^9$  per cubic centimeter. In approximately spherical plasmas, single body-centered cubic (bcc) crystals or, in some cases, two or more bcc crystals having fixed orientations with respect to each other were observed. In some oblate plasmas, a mixture of bcc and face-centered cubic ordering was seen. Knowledge of the properties of one-component plasma crystals is required for models of white dwarfs and neutron stars, which are believed to contain matter in that form.

Plasmas, the ionized states of matter, are usually hot and gaseous. However, a sufficiently cold or dense plasma can be liquid or solid. A one-component plasma (OCP) consists of a single charged species embedded in a uniform, neutralizing background charge (1). Aside from its intrinsic interest

as a simple model of matter, the OCP may be a good model for some dense astrophysical plasmas (2), such as the crusts of neutron stars or the interiors of white dwarfs, where the nuclei are embedded in a degenerate electron gas. According to calculations, a classical, infinite OCP freezes into a bcc lattice when the Coulomb coupling parameter

$$\Gamma \equiv \frac{1}{4\pi\epsilon_0} \frac{e^2}{a_{\text{WS}} k_B T} \quad (1)$$

is approximately equal to 170 (3). Here,  $\epsilon_0$  is the permittivity of the vacuum,  $e$  is the charge of an ion,  $k_B$  is Boltzmann's con-

Time and Frequency Division, National Institute of Standards and Technology, Boulder, CO 80303, USA.

\*To whom correspondence should be addressed. E-mail: witano@nist.gov

†Present address: Frequency & Time Systems, Beverly, MA 01915, USA.

‡On leave from the Institute of Physics, University of Belgrade, Belgrade, Yugoslavia.